Erosion Analysis for the Carcass of Unbonded Flexible Pipes

Jianxing Yu
Tianjin University
Haoda Li (lihaoda@tju.edu.cn)
Tianjin University
Yang Yu
Tianjin University
Xin Liu
Tianjin University
Weipeng Xu
Tianjin University
Pengfei Liu
Tianjin University
Ruoke Sun
Tianjin University

Research Article

Keywords: Erosion Analysis, Unbonded Flexible Pipes, pipelines

Posted Date: January 5th, 2022

DOI: https://doi.org/10.21203/rs.3.rs-1194029/v1

Erosion Analysis for the Carcass of Unbonded Flexible Pipes

Jianxing Yu[1,2], Haoda Li[1,2*], Yang Yu[1,2], Xin Liu[1,2], Weipeng Xu[1,2], Pengfei Liu[1,2], and Ruoke Sun[1,2]

[1]State Key Laboratory of Hydraulic Engineering Simulation and Safety, Tianjin University, Tianjin 300072, China
[2]Tianjin Key Laboratory of Port and Ocean Engineering, Tianjin University, Tianjin 300072, China
[*]lihaoda@tju.edu.cn
[+]these authors contributed equally to this work

ABSTRACT

At present, unbonded flexible pipes (UFPs) are widely used in ocean engineering for oil exploitation. In practice, erosion will lead to premature failure of pipelines. There is a lack of researches on the erosion of interlock carcass of UFPs. As the authority in the field of offshore engineering, DET NORSKE VERITAS(DNV) suggested a way to estimate the erosion rate of pipes, however, it does not study the erosion mechanism of UFPs in detail and the relevant parameters are not specified. This paper modifies erosion prediction of UFPs based on a user defined Fortran subroutine. A series of CFD simulations have been conducted, and three widely used erosion models were used for comparative verification. The effect of geometric shape on erosion rate has been carefully studied. and the effect of velocity, particle size, and concentration are also studied to verify the reliability of the improved model.

Introduction

Flexible pipes are important components of offshore platforms, especially in offshore oil engineering and deep-sea mining industry. As the depletion of offshore and shallow onshore oil resources, it becomes more and more important to explore the deep sea in which submarine pipelines as the foundation of marine engineering have been more widely used[1]. Among them, UFPs play an increasingly important role due to the excellent tensile and compression performance brought by their multilayer composite structures[2].

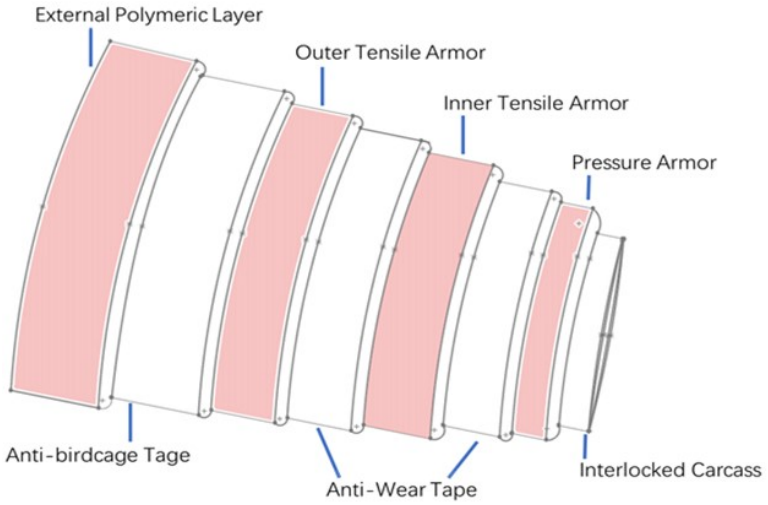

Figure 1. Typical unbonded flexible pipe cross-section.

The typical structural is shown in Figure 1. UFPs usually consist of eight layers. They are polymeric layers, including anti-wear tapes, fluid barriers and outer sheath, provide leak-proof capacity in respect. In the meantime, they can reduce the friction abrasion between metallic layers and protect pipes against seawater ingress in the annulus[3]. The sealing is provided by the concentric polymeric layers. And the internal and external pressure is resisted by the interlocked metallic layers when the

axial loads and torsion are carried by the helically wound tensile armour wire layers[4]. Generally, the curvature of the buoyancy segment is smaller than typical riser structures. The comparison results of the two forms are shown in the Figure 2.

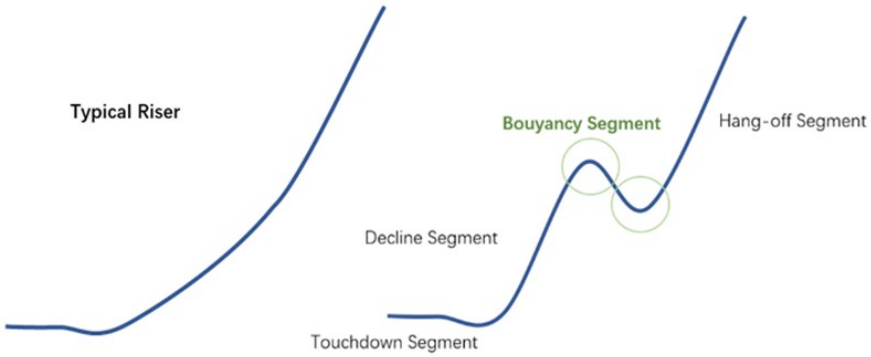

Figure 2. Typical riser and lazy wave riser.

Erosion in pipes with smooth surface has been studied a lot for more than 50 years, especially of 90-degree bends and T-branch pipes. Finnie[5]was the first to propose erosion model and Oka erosion model was proposed[6] later. In recent years, Homicz[7] performed simulations of flow in a constant radius smooth 90° bend. Yang[8] investigated the relationship between slurry flow velocity and confirmed the effects of impact angle on electrode surface status and E–C rate. Then Cheng[9–12] discussed erosion-accelerated in flow systems. Arun[13,14] investigated the fluid dynamics and wall erosion characteristics in 90-degree circular bends. Wang[15–17] developed an erosion equation with the consideration of applied stress for the first time and simulated the erosion of high-pressure pipe bends considering fluid-induced stress. Peng and Cao[18–20] analysed the erosion profile and explained the erosion mechanism through an experimental facility and CFD simulation. Kumar[21] studied the erosion of AISI 316 pipe bend and the optimal distance of pacing the vane under different angles and velocities. Liu and Zhang[22–24] derived a theoretical solution to the movement and erosion of solid particles in a bend and proposed a simplified CFD-based erosion prediction procedure to calculate the erosion rates in elbows for annular flow. Kannojiya[25] simulated erosion using ANSYS CFX and the results can be employed in industrial flow applications.

From previous research[26], erosion in pipes with smooth inner surfaces can be easily predicted with industry-standard prediction methodologies. However, there is little information available on erosion of UFPs[27] which has interlock carcasses existing on the inner surface. Not all bending pipes have smooth inner wall, and there is a lack of research on erosion of single-ply bellows such as flexible pipes. To date, few works have addressed the erosion of the carcass. For example, DET NORSKE VERITAS has not given the specific value of GF in the assessment of UFPs. Only a minimum of GF for the leading edge of the interlock carcass was proposed and the specific erosion mechanism is not clear.

The present work shows that the value of erosion calculated by the DNV theory is too small, which may cause serious safety problems in practical projects. Therefore, a series of numerical simulations were done to develop an improved model in this paper, and the predicted value was compared with the numerical simulation results. Finally, the variation of erosion rate with geometric shape was investigated to determine function value of the improved model.

Results

In this paper, the erosion rate for the carcass of UFPs has been firstly analyzed and results have been compared with pipes with smooth inner surface using several erosion models. In order to verify new model, the effects of velocity of particles, size of particle and the concentration of particles have been studied. In the end, modification of the convex parameters is provided. It can be concluded that:

The simulation results of the new model under various conditions are more accurate than those of DNV specification.

It has been found that erosion rate increases with fluid velocity increasing, concentration and size of particles. In all cases, the erosion rate of DNV model is slightly greater than that of Tabakoff model. When the velocity is low, the predicted results of Finnie model are in good agreement with other groups. As the velocity increases, the erosion difference increases significantly.

As the roughness of convex structure increases, the erosion rate increases firstly. When the length of pits is close to radius of arcs, the erosion rate comes to maximum and then decreases. The improved model was summarized.

Discussion

To validate the presently adopted DNV standard, a separate numerical study was carried out on smooth pipes, which was compared with each other. The CFD analysis results of erosion rate density, streamlines and particles tracking of the smooth pipes and UFPs are shown in Figure 3. In smooth-faced pipes, the erosion rate distribution varies between $4.156{*}10^{-8} kg/(m^2 * s)$ and $8.2671^{-6} kg/(m^2 * s)$. The erosion rate by using Finnie and Tabakoff model have been calculated from $1.537 * 10^{-8} kg/(m^2 * s)$ to $1.254 * 10^{-4} kg/(m^2 * s)$. The maximum erosion is near the outside profile the same as a standard 90° bend. The velocity of initial particles are perpendicular to the inlet surface which are uniformly distributed. From the statistical conclusion of the experiment, the maximum erosion area is strip equidistant distribution and is located outside pipes. For UFPs, an obvious conclusion is that the site of erosion is located at the innermost part of the carcass and velocity of particles near pipes decreases as shown in Figure 3.

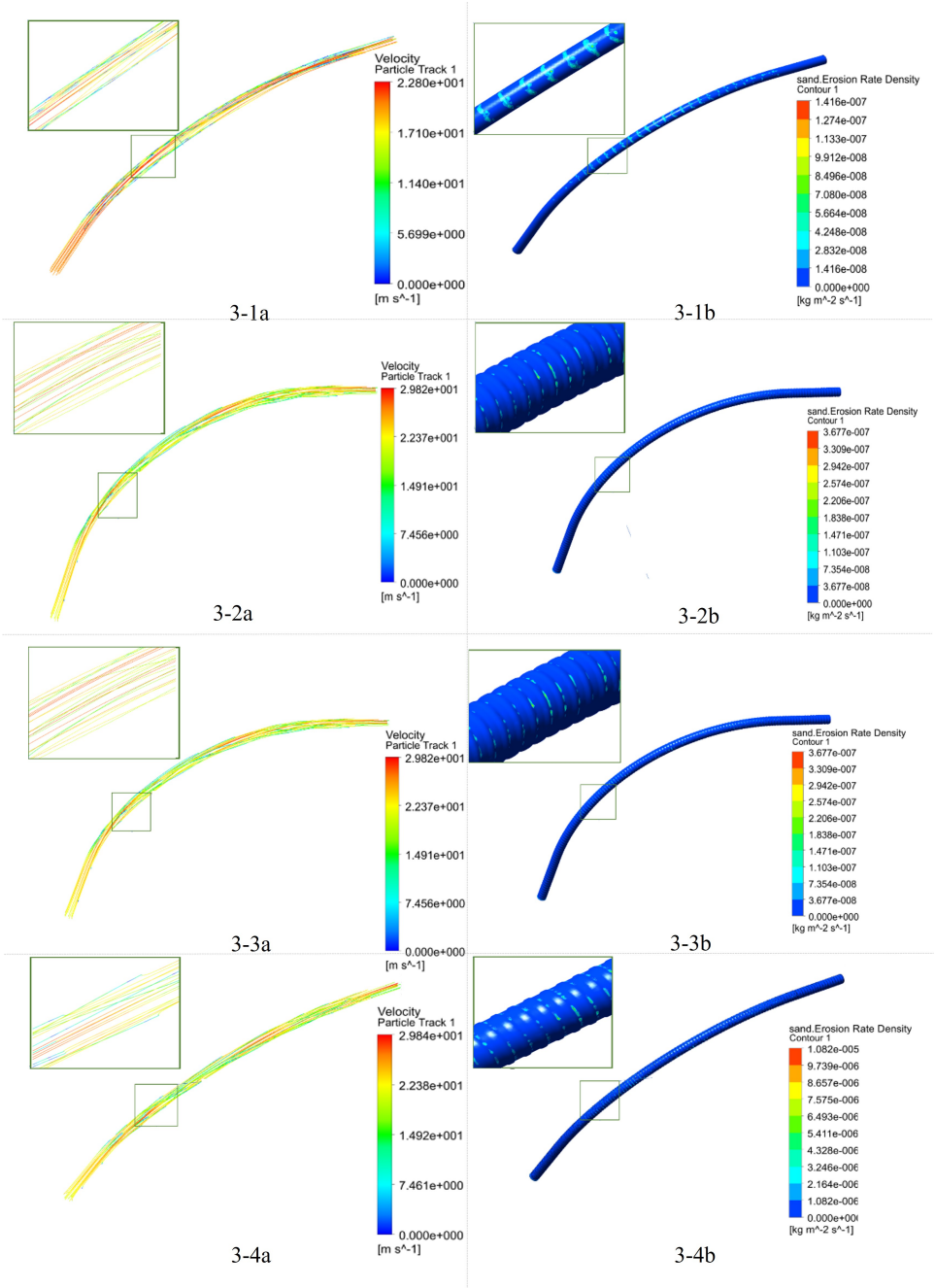

Figure 3. Particle collision and erosion results.

Effect of Pressure

These four sets of graphs are the erosion results at 20m/s. As the blue darkens, the erosion rate decreases. The most severe corrosion occurs in the pit, which is the result of multiple rebound particles in it. According to the particle trajectory graphs, we can find that the number of particle collisions in UFPs is significantly greater than that in the smooth pipes, which explains the large erosion rate of UFPs. The pressure distribution of the four models when the speed is adjusted to 20m/s is shown in Figure 4, which depicts the pressure distribution in UFPs. It is shown that pressure in outer-side elbow is higher than that in the inner-side elbow.

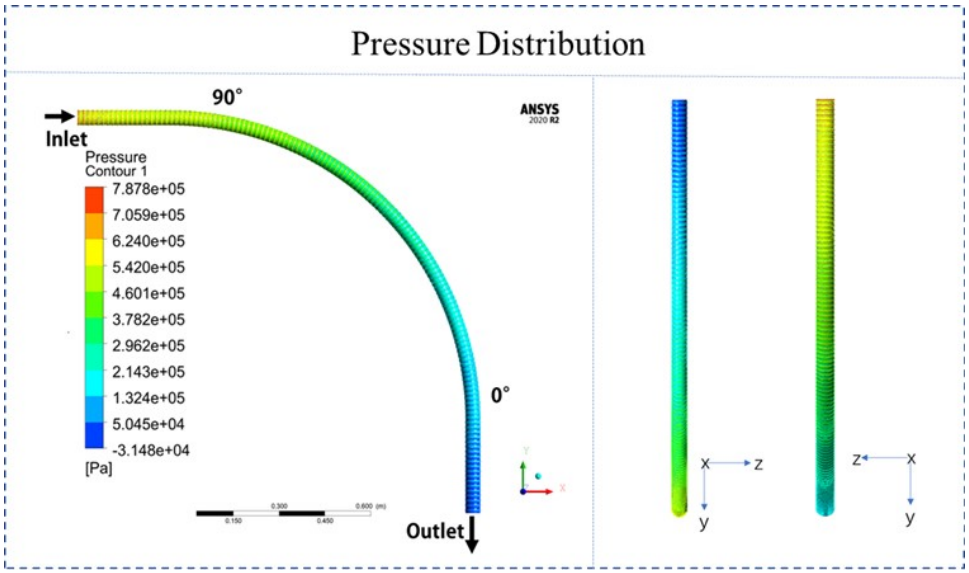

Figure 4. Pressure distribution in UFPs.

Figure 5 depicts the velocity distribution in different cross-sections. And angle refers to the position of the pipes in figures, which is also marked in Figure 5. Green areas have lower speeds and red areas have higher speeds. There is higher speed in the inner side elbow.

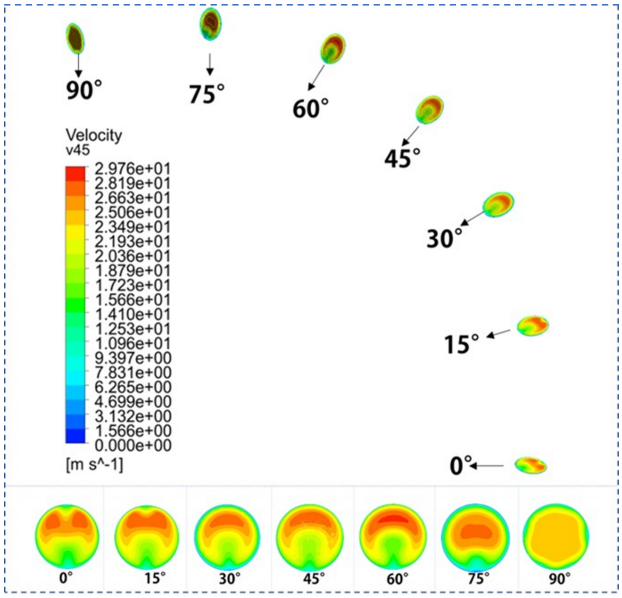

Figure 5. Speed distribution in UFPs.

For the new computation model, different geometry parameters will be discussed in this section. From figures above, it can be found that the main eroded part of UFPs is the pit.

In this part, its length has been changed to decrease value of erosion. As shown in Fig.11, when the length of pits is less than 11mm, the erosion rate increases with the increase of length. However, when the length of pits is greater than 11mm, the erosion rate decreases with the increase of it. When the length is small enough, the outer length is larger and the inner surface is smoother. Similarly, when its large enough, inner surface is rougher. It is easy to find that when its value between 10mm and 35mm, the probability of particle collision is the highest, leading to the most erosion rate. Therefore, the optimal length of pit should be evaluated at both ends of the curve.

In the meantime, Figure 6 illustrates f(Le/r) is an unimodal function. The sensitivity analysis in the following part will also prove this point.

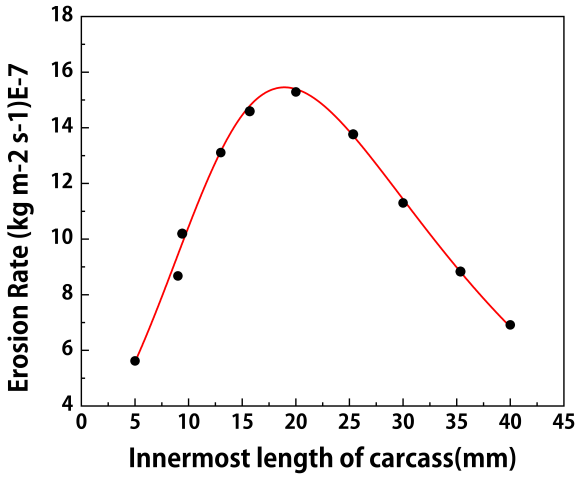

Figure 6. Erosion under Different Innermost Length.

Effect of impact velocity

Impact velocity is compared to pipes with a smooth inner surface, the maximum erosion result of UFPs is greater. And the difference increases as the velocity increases. The erosion results under four conditions were compared as shown in Figure 7.

In the legend, 'DNV', 'Tabakoff' and 'Finnie' means that the result is obtained by 'DNV', 'Tabakoff' and 'Finnie' models. In the legend, '0.5 Improved' means erosion results of pipes with smooth surfaces with improved model and the number in front of it represents coefficient of f(Le/r).

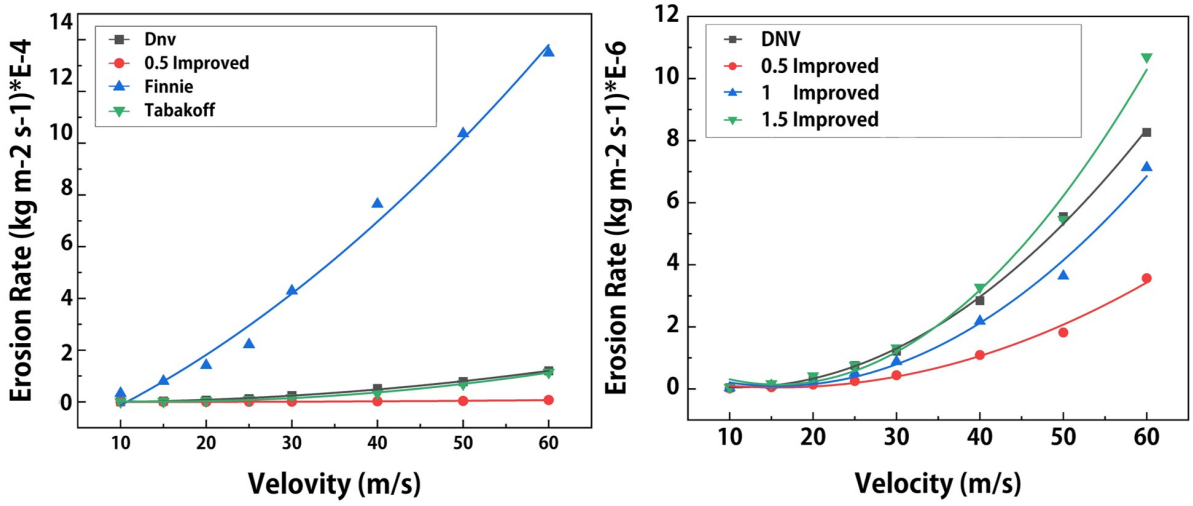

Figure 7. Erosion results under 5 working conditions(left) and different model parameters(right).

It can be seen from Figure 7 the erosion rate of Finnie model is the maximum under the same velocity condition. Consistent with the experiment of Wang[28], the rate of DNV model is higher than that of Tabakoff model.

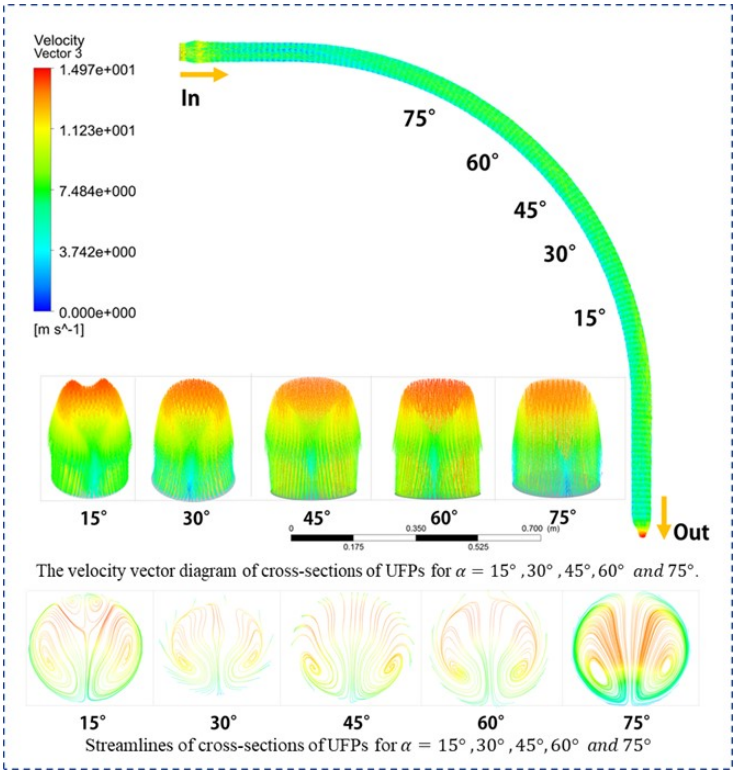

Figure 8. The velocity vector diagram of cross-sections of UFPs and streamlines.

Figure 8 shows that there are low-speed zone exists on the outer side of the UFPs. It depicts speed of the central part is higher than that of the outer part in each cross-section.

Conclusions can be drawn that the erosion results of DNV model is about equal to that of the improved model. When the velocity increases, the difference of erosion rate between DNV model and 1.5 improved model is not significant. It is safe to use only when its value is greater than the specification value.Referring to the conversion of DNV formula, we found that when the velocity was 10-60m/s,only the erosion rate of '1.5 Improved model' meets the specification.

Effect of Particle Concentration

With the increase of particle concentration, the erosion rate increases almost linearly. Consistent with the above conclusions[28], the erosion rate of DNV model at various concentrations was slightly higher than Tabakoff model. A conclusion can be drawn from Figure 9 that improved model is applicable to the erosion rate prediction under various particle size gradients and the value of $f(\frac{Le}{r})$ is 1.4.

Based on the discussion above, $f(\frac{Le}{r})$ should take the maximum of a reasonable value in order to make the rapid prediction more accurate under the circumstance of ensuring safety.

Effect of Particle Size

Erosion rate density increases to a maximum value when the value of particle diameter is 500μm. The rate rises with the increase of particle size as shown in Figure 10.

Consistent with the above results, the erosion rate of UFPs is higher than that of pipes with smooth surfaces. Among three parameters, The maximum value is obtained under the condition that DNV model is used. Only when the value is lower than the standard value can it operate safely and pass the institution inspection .The coincidence rate between '1 Improved' model and DNV curves is very high, ans some of the lower values are danger points. Hence, the most appropriate value of $f(\frac{Le}{r})$ is 1.75.

Modification of the Convex Parameters

Considering all cases, the following conclusion can be reached. Because the inner wall of UFPs is uneven, the number of collisions between particles and walls increases significantly. With the number of collisions increases, the erosion rate will increase significantly. Therefore, the erosion rate of UFPs is higher than that of smooth pipes.

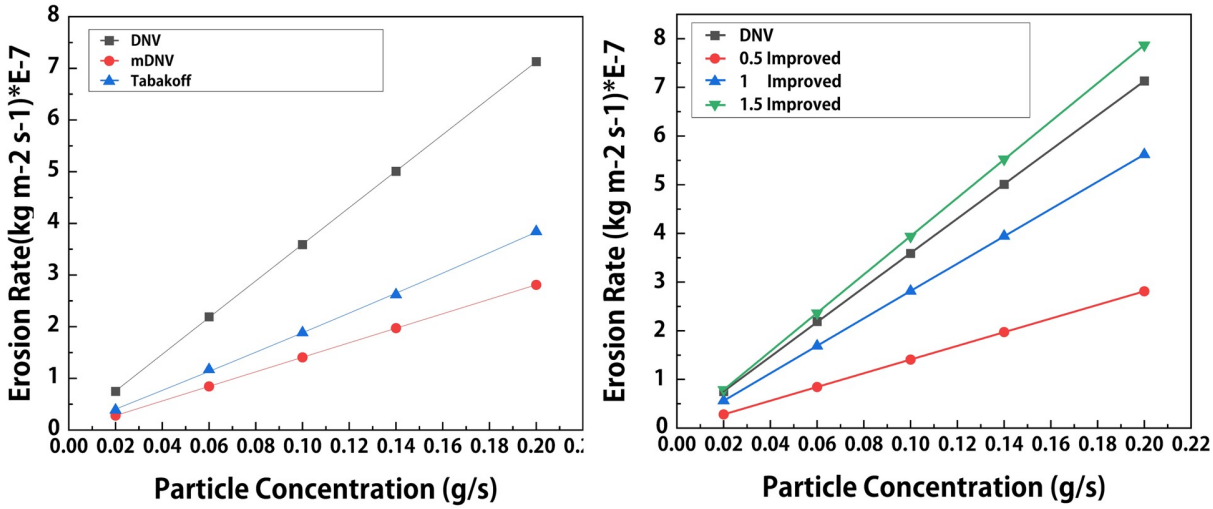

Figure 9. Erosion results by using different model parameters.

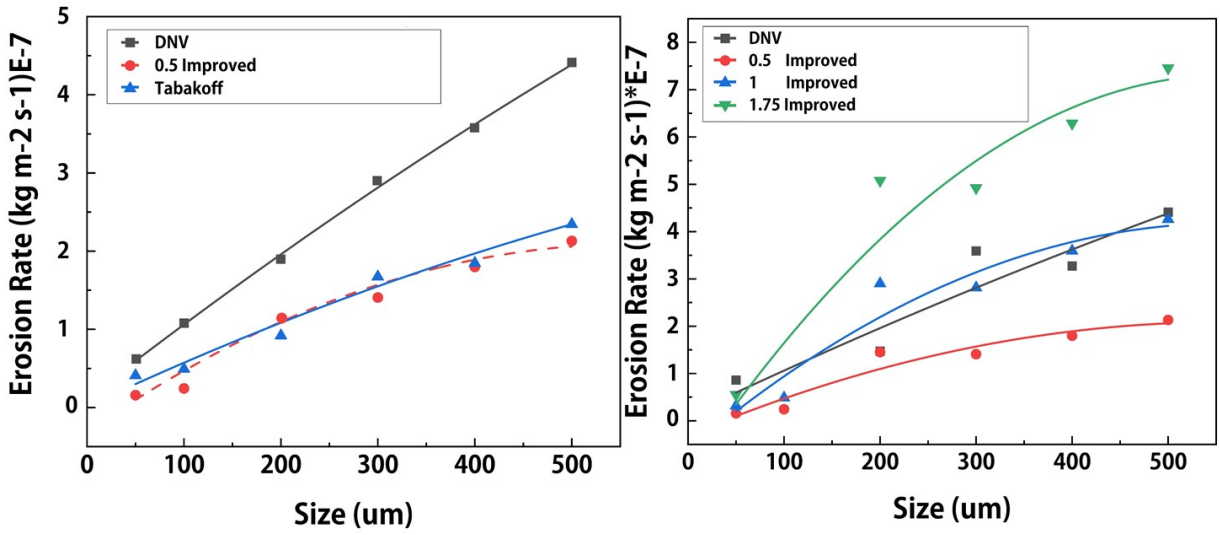

Figure 10. Erosion results under different model parameters.

In order to satisfy the needs of accuracy and safety at the same time, considering all cases above, the value of convex parameters should take the minimal maximum. Therefore, it is suggested that the value of $\frac{Le}{r}$ should be modified to 1.75.

Methods

Due to the entrainment of a large number of particles in the multiphase flow, the innermost interlock carcass will be eroded. Erosion depends on surface, granular flow properties and erodent. In general, the curvature radius of UFPs are greater than pipes with smooth inner surfaces. Up to now, most of the researches are focused on tubes with smooth inner surfaces. The curved area of interlock carcass inside the flexible pipes is cratering, which will have a completely different erosion result from the previous studies.

The sand particles are mixed with petroleum, making the solution more viscous. The oil slurry is usually transported to FPSO (Floating Production, Storage and Offloading Unit) or the desired place using pipelines[29,30]. A schematic of particle erosion is shown in Figure 11. If angles between 0-18.42°, sliding wear dominates, otherwise, impact wear dominates[31]. And for most of the curved made by the standard cast iron, if angles between 40–45°, impact wear dominates[32].

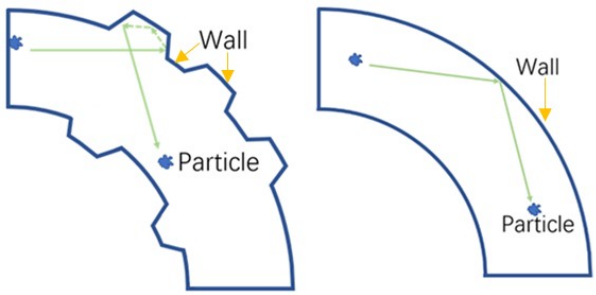

Figure 11. Erosion Sketch of UFPs and Conventional Pipes.

Interlock Carcass Physical Parameters

The configuration of carcass profiles is shown in Figure 12. Since we only focus on the internal flow field in this paper, its outer profile was simplified by taking the centre line as the axis and the inner side as the edge line. The simplified edges are highlighted in Figure 12. The comparison results of the two pipes are shown in the Figure 13.

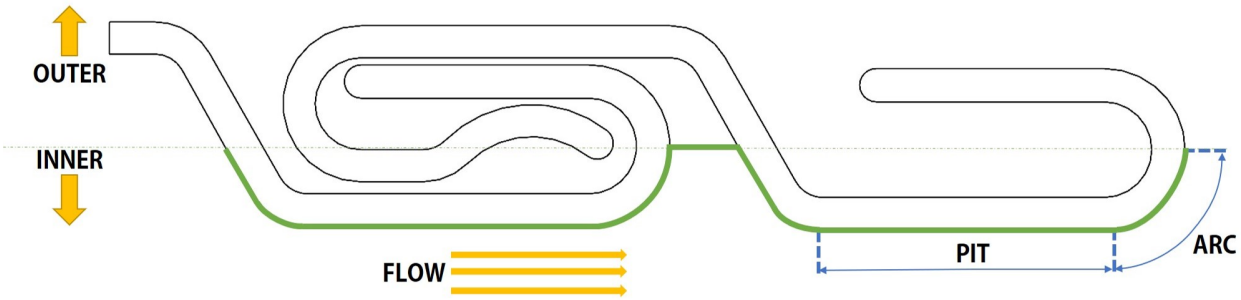

Figure 12. Carcass Profile Configuration.

According to the API specification[33], the model parameters are shown in Table 1.

Parameters	Value
Inlet and Outlet Angle	90 deg
Max Inner Diameter	50 mm
Inlet Length	300 mm
Outlet Length	300 mm
Radius of Curvature	1000 mm

Table 1. Interlock Carcass Physical Parameters.

Erosion Model

There are many types of erosion models that can be used to study pipelines. An improved model is proposed below. Through the calculation of pipes with smooth surfaces, the equivalent erosion rate of UFPs can be obtained. In order to compared with other models, three models have been programmed by Fortran into ANSYS-CFX for comparison. The improved model takes it into account that the influence of the convex structures in the interlock carcass of UFPs. With the new model, we only need to calculate erosion rate of the pipes with smooth surfaces, the UFPs erosion results can be obtained.

The improved model is shown below:

$$E = f(\tfrac{Le}{r}) * \tfrac{K*F(\alpha)*U_P^n}{\rho_t * A_t} * G * C_1 * GF * M_P * 10^3$$
$$f(\tfrac{Le}{r}) = G_1 * (\tfrac{Le}{r})^2 + G_2 * \tfrac{Le}{r} + G_3$$

Where $f(\frac{Le}{r})$ represents the influence of the convex structure of the skeleton layer on the erosion results. Le means the length of pit in Figure 12, r represents the radius is the radius of the arcs,$G_1G_2G_3$ are convex parameters related to convex

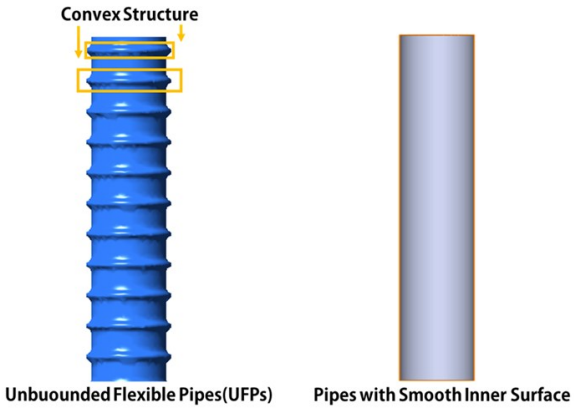

Figure 13. Comparison of Two Kinds of Pipes.

structures, K represents the material erosion constant, $F(\alpha)$ is the function characterizing ductility of material,U_P represents the particle impact velocity, G represents corrections function for particle diameter, C_1 represents geometry factor, M_P is the mass of sand, ρ_t means the density of target material, A_t is the impact area of particles, some relevant properties are shown in Table 2.

Parameters	Symbols	Values
The Model Geometry Factor	C_1	2.5
The Unit Conversion Factor	C_{unit}	$3.15 * 10^{10}$
The Geometry Factor	GF	2

Table 2. Parameters of DNV Model.

In this paper, Finnie and Tabakoff erosion models were used to derived the improved model, both of which are widely used in industry. Detailed information of these two models are shown as follows:

Finnie model

$$E = kV_p^n f(\alpha)$$
$$f(\alpha) = sin(2\alpha) - 3 * sin^2\alpha \quad \text{when } 3 * tan\alpha \leq 1$$
$$f(\alpha) = \tfrac{1}{3} \quad \text{when } 3 * tan\alpha > 1$$

where $n = 2$, V_p is the particle impact velocity, α is the particle impact angle. In the Ansys CFX, we use $V_0 = (\sqrt[n]{\frac{1}{k}})$ to simulate different materials.

Tabakoff model

Relative parameters are made to be tally with the actual situation [43]. In this model, the erosion rate is determined from the following relation:

$$E = f(\alpha)(\tfrac{V_P}{V_1})^2 cos^2\alpha(1 - R_T^2) + f(V_{PN})$$
$$f(\alpha) = [1 + k_2 * k_{12} * sin(\tfrac{\pi * \gamma}{2 * \gamma_0})]^2$$
$$f(V_{PN}) = (\tfrac{V_P}{V_2} sin\gamma)^4$$

where $R_T = 1 - \frac{V_P}{V_3} sin\gamma$ and the value of k_{12} k_2 V_1 V_2 *and* V_3 are shown in Table 3

Particles tracking model

In order to predict the trajectory of particles in UFPs and to figure out the erosion path, integrating the solution of force balance equation is needed. The equation is shown in the following:

$$F_D(v_L - v_S) + g\tfrac{rho_s - rho_L}{rho_S} + F = \tfrac{\partial u_s}{\partial t}$$

where F_D represents the drag force, v_L means the velocity of liquid, v_L means the velocity of solid, F represents the force per unit paticle mass, g means gravity, rho_s and rho_L are the density of solids and fluids.

Parameters	Symbols	Values
Ref Velocity 1	V_1	51[m/s]
Ref Velocity 2	V_2	$3.15 * 10^{10}$[m/s]
Ref Velocity 3	V_3	2 [m/s]
Angle of Maximum Erosion	γ_0	25[deg]
Ref k	k_{12}	$1.321448 * 10^{-1}$

Table 3. Parameters of Erosion Model.

References

1. Guha, I., White, D. J. & Randolph, M. F. Parametric solution of lateral buckling of submarine pipelines. *Appl. Ocean. Res.* **98**, 102077, DOI: https://doi.org/10.1016/j.apor.2020.102077 (2020).
2. Zhang, Y., Wang, Z., Yang, Q. & Wang, H. Numerical analysis of the impact forces exerted by submarine landslides on pipelines. *Appl. Ocean. Res.* **92**, 101936, DOI: https://doi.org/10.1016/j.apor.2019.101936 (2019).
3. Li, X., Vaz, M. A. & Custodio, A. B. Analytical and experimental studies on flexible pipes tensile armors lateral instability in cyclic bending. *Mar. Struct.* **67**, 102630.1–102630.24, DOI: https://doi.org/10.1016/j.marstruc.2019.05.008 (2019).
4. Li, X. & Vaz, M. A. Analytical model for lateral instability of quasi-rectangular or circular armor wires in flexible pipes and umbilicals. *Ocean. Eng.* **190**, 106423–, DOI: https://doi.org/10.1016/j.oceaneng.2019.106423 (2019).
5. Finnie, I. Erosion of surfaces by solid particles. *Wear* **3**, 87–103, DOI: https://doi.org/10.1016/0043-1648(60)90055-7 (1960).
6. Oka, Y. I., Ohnogi, H., Hosokawa, T. & Matsumura, M. The impact angle dependence of erosion damage caused by solid particle impact. *Wear* **203**, 573–579, DOI: https://doi.org/10.1016/S0043-1648(96)07430-3 (1997).
7. Homicz, G. F. Computational fluid dynamic simulations of pipe elbow flow. *SAND* 1–29, DOI: https://doi.org/10.2172/919140 (2004).
8. Yang, Y. & Cheng, Y. F. Parametric effects on the erosion–corrosion rate and mechanism of carbon steel pipes in oil sands slurry. *Wear* **276-277**, 141–148, DOI: https://doi.org/10.1016/j.wear.2011.12.010 (2012).
9. Cheng, F. Y. Erosion-accelerated corrosion in flow systems: the behavior of aluminum alloys in automotive cooling systems - sciencedirect. *Tribocorrosion Passiv. Met. Coatings* 475–497, DOI: https://doi.org/10.1016/B978-1-84569-966-6.50017-8 (2011).
10. Dong, C. F., Xiao, K., Li, X. G. & Cheng, Y. F. Erosion accelerated corrosion of a carbon steel–stainless steel galvanic couple in a chloride solution. *Wear* **270**, 39–45, DOI: https://10.1016/j.wear.2010.09.004 (2010).
11. Zhang, G. A., Xu, L. Y. & Cheng, Y. F. Investigation of erosion–corrosion of 3003 aluminum alloy in ethylene glycol–water solution by impingement jet system. *Corros. Sci.* **51**, 283–290, DOI: https://doi.org/10.1016/j.corsci.2008.10.026 (2009).
12. Niu, L. & Cheng, Y. F. Synergistic effects of fluid flow and sand particles on erosion–corrosion of aluminum in ethylene glycol–water solutions. *Wear* **265**, 367–374, DOI: https://doi.org/10.1016/j.wear.2007.11.007 (2008).
13. Arun, G., Babu, S. P. K., Natarajan, S. & Kulasekharan, N. Numerical predictions of fluid dynamics and wall erosion characteristics in a circular 90 deg. pipe bend with single and multi mitred joint. *Mater. Today: Proc.* **27**, DOI: https://doi.org/10.1016/j.matpr.2019.09.077 (2019).
14. Arun, G., Kumaresh Babu, S., Natarajan, S. & Kulasekharan, N. Study of flow behaviour in sharp and mitred pipe bends. *Mater. Today: Proc.* **27**, 2101–2108, DOI: https://doi.org/10.1016/j.matpr.2019.09.076 (2020).
15. Wang, H. *et al.* Statistical characterization of irregular fine sand particles and numerical simulation of the corresponding 2-d and 3-d models. *J. Tianjin Univ. Technol.* DOI: https://doi.org/10.11784/tdxbz201805005 (2019).
16. Wang, H., Yu, Y., Yu, J., Wang, Z. & Li, H. Development of erosion equation and numerical simulation methods with the consideration of applied stress. *Tribol. Int.* **137**, 387–404 (2019).
17. Wang, H., Yu, Y., Yu, J., Xu, W. & Yu, S. Numerical simulation of the erosion of pipe bends considering fluid-induced stress and surface scar evolution. *Wear* **s 440–441**, DOI: https://doi.org/10.1016/j.wear.2019.203043 (2019).
18. Peng, W. & Cao, X. Numerical prediction of erosion distributions and solid particle trajectories in elbows for gas-solid flow. *J. Nat. Gas Sci. Eng.* **30**, 455–470, DOI: https://doi.org/10.1016/j.jngse.2016.02.008 (2016).

19. Peng, W. & Cao, X. Numerical simulation of solid particle erosion in pipe bends for liquid–solid flow. *Powder Technol.* **294**, 266–279, DOI: https://doi.org/10.1016/j.powtec.2016.02.030 (2016).

20. Peng, W., Cao, X., Hou, J., Xu, K. & Xing, S. Experiment and numerical simulation of sand particle erosion under slug flow condition in a horizontal pipe bend. *J. Nat. Gas Sci. Eng.* 103175, DOI: https://doi.org/10.1016/j.jngse.2020.103175 (2020).

21. Kumar, J., Baghel, Y. K., Tiwari, G., Rawat, A. & Patel, V. K. Effect of swirl vanes angle on erosion behaviour of aisi 316 pipe bend - sciencedirect. *Mater. today: proceedings* DOI: https://doi.org/10.1016/j.matpr.2020.01.026 (2020).

22. Liu, M., Liu, H. & Zhang, R. Numerical analyses of the solid particle erosion in elbows for annular flow. *Ocean. Eng.* **105**, 186–195, DOI: https://doi.org/10.1016/j.oceaneng.2015.06.024 (2015).

23. Zhang, R., Zhu, D., Liu, H. & Liu, Y. Random process of particle-wall collision and its application in numerical simulation of solid particle erosion. *Wear* **452-453**, 203288, DOI: https://doi.org/10.1016/j.wear.2020.203288 (2020).

24. Zhao, Y., Yan, C., Wang, X., Liu, H. & Zhang, W. Uncertainty and sensitivity analysis of sst turbulence model on hypersonic flow heat transfer. *Int. J. Heat Mass Transf.* **136**, 808–820, DOI: https://doi.org/10.1016/j.ijheatmasstransfer.2019.03.012 (2019).

25. Kannojiya, V., Deshwal, M. & Deshwal, D. Numerical analysis of solid particle erosion in pipe elbow. *Mater. Today: Proc.* **5**, 5021–5030, DOI: https://doi.org/10.1016/j.matpr.2017.12.080 (2018).

26. Helgaker, J. F. *et al.* Large-scale erosion testing of an unbonded flexible pipe. *SPE J.* DOI: https://doi.org/10.2118/181761-PA (2017).

27. Drumond, G. P., Pasqualino, I. P., Pinheiro, B. C. & Estefen, S. F. Pipelines, risers and umbilicals failures: A literature review. *Ocean. Eng.* **148**, 412–425, DOI: https://doi.org/10.1016/j.oceaneng.2017.11.035 (2018).

28. Wang, S. M., Liu, H. X., Zhang, R. & Liu, M. Y. Numerical simulations of sand erosion in pipelines and evaluations of solid particle erosion equations. *The Ocean. Eng.* **32**, 49–59, DOI: https://doi.org/10.16483/j.issn.1005-9865.2014.01.005 (2014).

29. Bruschi, R., Vitali, L., Marchionni, L., Parrella, A. & Mancini, A. Pipe technology and installation equipment for frontier deep water projects. *Ocean. Eng.* **108**, 369–392, DOI: https://doi.org/10.1016/j.oceaneng.2015.08.008 (2015).

30. Gonzalez, G. M., Sousa, J. D. & Sagrilo, L. A modal finite element approach to predict the lateral buckling failure of the tensile armors in flexible pipes. *Mar. Struct.* **67**, 102628.1–102628.29, DOI: https://doi.org/10.1016/j.marstruc.2019.05.006 (2019).

31. Noon, A. A. & Kim, M. H. Erosion wear on centrifugal pump casing due to slurry flow. *Wear* **364-365**, 103–111, DOI: https://doi.org/10.1016/j.wear.2016.07.005 (2016).

32. Arabnejad *et al.* Development of mechanistic erosion equation for solid particles. *Wear: an Int. J. on Sci. Technol. Frict. Lubr. Wear* **332/333**, 1044–1050, DOI: http://dx.doi.org/10.1016/j.wear.2015.01.031 (2015).

33. Zhang, Y. N., Lan, L. I., Song, P. N. & Meng, D. J. Analysis method of corrosion and erosion on the carcass of unbonded flexible pipe. *China Offshore Platf.* (2015).

Acknowledgements

This project was supported by the National Natural Science Foundation of China (Grant No.51879189), Project of ministry of industry and information technology(Grant No. MC-201917-C09) and National Natural Science Foundation of China (Grant No. 52071234).

Author contributions statement

Jianxing Yu and Haoda Li conceived the article, Yang Yu and Xin Liu did numerical simulations, Weipeng Xu and Pengfei Liu analyzed the experimental data, Ruoke Sun analysed the results. All authors reviewed the manuscript.

Additional information

Competing interests (mandatory statement). The authors declare that they have no known competing financial interests or personal relationships that could have appeared to influence the work reported in this paper.